Published in final edited form as:
J Neurol Sci. 2014 July 15; 342(0): 152–161. doi:10.1016/j.jns.2014.05.019.

Lateralization of Temporal Lobe Epilepsy using a Novel Uncertainty Analysis of MR Diffusion in Hippocampus, Cingulum, and Fornix, and Hippocampal Volume and FLAIR Intensity

Mohammad-Reza Nazem-Zadeh[1], **Jason M. Schwalb**[2], **Kost V. Elisevich**[3], **Hassan Bagher-Ebadian**[1,4], **Hajar Hamidian**[1,5], **Ali-Reza Akhondi-Asl**[6], **Kourosh Jafari-Khouzani**[1,7], and **Hamid Soltanian-Zadeh**[1,8]

Mohammad-Reza Nazem-Zadeh: mohamadn@rad.hfh.edu; Jason M. Schwalb: jschwal1@hfhs.org; Kost V. Elisevich: kost.elisevich@spectrumhealth.org; Hassan Bagher-Ebadian: hbagher1@hfhs.org; Hajar Hamidian: nasimh@rad.hfh.edu; Ali-Reza Akhondi-Asl: alireza.akhondi-asl@childrens.harvard.edu; Kourosh Jafari-Khouzani: kjafari@nmr.mgh.harvard.edu; Hamid Soltanian-Zadeh: hamids@rad.hfh.edu

[1]Radiology and Research Administration Department, Henry Ford Hospital, Detroit, MI, 48202, USA

[2]Neurosurgery Department, Henry Ford Hospital, Detroit, MI, 48202, USA

[3]Department of Clinical Neurosciences, Spectrum Health Medical Group, Grand Rapids, MI, 49503, USA

[4]Neurology Department, Henry Ford Hospital, Detroit, MI, 48202, USA

[5]School of Computer Science, Wayne State University, Detroit, MI, 48202, USA

[6]Computational Radiology Laboratory, Dept. of Radiology, Children's hospital, Boston, MA 02115, USA

[7]Athinoula A. Martinos Center for Biomedical Imaging, Department of Radiology, Massachusetts General Hospital, Harvard Medical School, Boston, MA, USA

[8]CIPCE, School of Electrical and Computer Engineering, University of Tehran, Tehran, Iran

Abstract

Purpose—To analyze the utility of a quantitative uncertainty analysis approach for evaluation and comparison of various MRI findings for lateralization of epileptogenicity in mesial temporal lobe epilepsy (mTLE), including novel diffusion-based analyses.

Corresponding Author: Mohammad-Reza Nazem-Zadeh, Radiology and Administration Departments, Henry Ford Hospital, Detroit, MI 48202, USA, mohamadn@rad.hfh.edu, Phone: (313) 874-4349.

Competing interests: None

Ethics approval:
Ethics approval was provided by Henry Ford Health System Institutional Review Board, Detroit, Michigan, USA.

Methods—We estimated the hemispheric variation uncertainty (HVU) of hippocampal T_1 volumetry and FLAIR (Fluid Attenuated Inversion Recovery) intensity. Using diffusion tensor images of 23 nonepileptic subjects, we estimated the HVU levels of mean diffusivity (MD) in the hippocampus, and fractional anisotropy (FA) in the posteroinferior cingulum and crus of fornix. Imaging from a retrospective cohort of 20 TLE patients who had undergone surgical resection with Engel class I outcomes was analyzed to determine whether asymmetry of preoperative volumetrics, FLAIR intensities, and MD values in hippocampi, as well as FA values in posteroinferior cingula and fornix crura correctly predicted laterality of seizure onset. Ten of the cohort had pathologically proven mesial temporal sclerosis (MTS). Seven of these patients had undergone extra-operative electrocorticography (ECoG) for lateralization or to rule out extra-temporal foci.

Results—HVU was estimated to be 3.1×10^{-5} for hippocampal MD, 0.027 for FA in posteroinferior cingulum, 0.018 for FA in crus of fornix, 0.069 for hippocampal normalized volume, and 0.099 for hippocampal normalized FLAIR intensity. Using HVU analysis, a higher hippocampal MD value, lower FA within the posteroinferior cingulum and crus of fornix, shrinkage in hippocampal volume, and higher hippocampal FLAIR intensity were observed beyond uncertainty on the side ipsilateral to seizure onset for 10, 10, 9, 9, and 10 out of 10 pathology-proven MTS patients, respectively. Considering all 20 TLE patients, these numbers were 18, 15, 14, 13, and 16, respectively. However, consolidating lateralization results of HVU analysis on these quantities by majority voting detected the epileptogenic side for 19 out of 20 cases with no wrong lateralization.

Conclusion—The presence of MTS in TLE patients is associated with an elevated MD value in the ipsilateral hippocampus and a reduced FA value in the posteroinferior subregion of the ipsilateral cingulum and crus of ipsilateral fornix. When considering all TLE patients, among the mentioned biomarkers the hippocampal MD had the best performance with true detection rate of 90% without any wrong lateralization. The proposed uncertainty based analyses hold promise for improving decision-making for surgical resection.

Keywords

Seizure Lateralization; Temporal Lobe Epilepsy; Mesial Temporal Sclerosis; Uncertainty Analysis; Diffusion MRI; Cingulum; Hippocampus; Fornix

1. Introduction

Mesial temporal lobe epilepsy (mTLE) is the most frequent type of refractory focal epilepsy. Among TLE structural abnormality syndromes, mesial temporal sclerosis (MTS) is the best predictor of successful surgery for epilepsy [1–4]. Patients with concordant EEG, seizure semiology, neuropsychology and MRI findings, such as atrophy on T1-weighted MR images and hyperintensity on MR Fluid Attenuated Inversion Recovery (FLAIR) of the hippocampus, ipsilateral to the side of seizure onset, do extremely well with resection of the mesial temporal structures [5–11]. However, many of the patients who do not have clear lateralization by preoperative visual inspection subsequently undergo implantation of intracranial electrodes to determine which mesial temporal lobe is epileptogenic [12]. Unfortunately, such implantation carries significant risks of infection, intracranial

hemorrhage and elevated intracranial pressure [13]. Prior research has shown that quantitative analysis may identify asymmetry that is not obvious by visual analysis [14]. Therefore, the need for implantation of intracranial electrodes could be obviated by exploiting quantitative lateralization methods. These methods include quantitative MRI analysis, ictal single-photon emission computed tomography (SPECT), positron emission tomography (PET), magnetoencephalography (MEG), MR spectroscopy, EEG-functional MRI, and Diffusion tensor imaging (DTI).

DTI has been investigated as a potential imaging modality for the detection of physiological and pathological changes in white and gray matter structures engaged in an epileptic network. Fractional anisotropy (FA) is a measure of fiber and myelin integrity, whereas mean diffusivity (MD) is a measure of bulk mobility of water molecules in tissues [15]. Most previous studies have reported more global bilateral FA and MD abnormalities in cases of unilateral TLE relative to matched regions in nonepileptic subjects [16–27]. Some have reported the ability of DTI to help identify which temporal lobe is epileptogenic by comparing variations between patients with MTS and nonepileptic controls [28–30]. However, this necessitates calibration with nonepileptic controls if a different MRI scanner is used. Prior studies have not compared the differences between homologous regions in each hemisphere in individual subjects, so that each patient can serve as his or her own control. While much previous work has focused on the temporal lobe, there is an opportunity to identify patients with unilateral MTS by examining extratemporal structures. A variety of imaging attributes, applied to both gray and white matter within such a network, have been used to distinguish the network's constituents and extent in one or both cerebral hemispheres [17, 19, 21, 22, 24, 25].

The cingulum, fornix, and hippocampus are integral components of Papez' circuit. There is evidence that they reflect activity of the mesial temporal structures [17, 18, 23, 24, 28, 29]. Their bilateral structure, parasagittal location and prominence make them suitable sites for comparative interhemispheric study of the hemispheric variation of diffusion indices. Our first hypothesis is that hemispheric variation of MD within the hippocampus and FA or MD within any of subregions of cingulum and crus of fornix could be used to confirm the laterality of mesial temporal epileptogenicity. The accrual of such quantitative imaging metrics enhances the confidence of clinical decision-making as it regards surgical candidacy and, in particular, the need for extraoperative ECoG.

In the analysis of hemispherical asymmetry of TLE bilateral structures, an interhemispheric variation of an imaging index in an individual patient must be beyond the minimum detectable value -hemispheric variation uncertainty (HVU)- to be interpreted as a true -significant variation [32, 33]. None of prior studies in the field which reported to observe a unilateral change in the TLE structures determined whether the observed change was beyond the uncertainty. Without such a determination, the trueness of observed changes should be considered with caution. Therefore, HVU analysis is of a significant importance especially for DTI measurements with quite large variability in diffusion indices [33]. Our second hypothesis is that a unified uncertainty-based analogy framework would be useful in comparing different TLE lateralization methods and modalities, including our proposed

diffusion-based lateralization methods, as well as hippocampal T_1 volumetry and FLAIR intensity analysis [7, 9].

2. Material and Methods

2.1.Human subjects and image acquisition

The current research study at Henry Ford Health System is federally regulated and approved by the Henry Ford Health System Institutional Review Board (IRB).

Out of 113 patients with TLE who underwent resection of the mesial temporal structures between June 1993 and June 2009, 100 patients achieved Engel class IA. We included only twenty of them (TLE cohort) in the study (10 females with age 41.8 ± 12.6 (mean ± standard deviation), 10 males with age 42.0 ± 12.5) which had preoperative DTI imaging. Seven of them had undergone extraoperative electrocorticography (ECoG) to determine epileptogenicity (left vs. right and/or temporal vs. extra-temporal). Ten were noted in pathology reports to have MTS (MTS cohort). Table 1 shows the characteristics of the patients.

Preoperative T1-weighted images of TLE patients were acquired on a 1.5T or a 3.0T MRI system (Signa, GE, Milwaukee, USA) using spoiled gradient echo protocol (SPGR). T1-weighted imaging parameters were TR/TI/TE=7.6/1.7/500 ms, flip angle=20°, voxel size=0.781mm×0.781mm×2.0 mm on 1.5T MRI, and TR/TI/TE=10.4/4.5/300 ms, flip angle=15°, voxel size=0.39mm×0.39mm×2.00 mm on 3.0T MRI.

Preoperative FLAIR images of TLE patients along were also acquired with imaging parameters of TR/TI/TE=10002/2200/119 ms, flip angle = 90°, voxel size = 0.781mm×0.781mm×3.0 mm on 1.5T MRI, and TR/TI/TE = 9002/2250/124 ms, flip angle = 90°, voxel size = 0.39mm× 0.39mm×3.00 mm on 3.0T MRI.

The diffusion weighted images (DWIs) along with a set of b_0 null images (with b-value = 0 s/mm^2) of TLE patients were acquired using echo planar imaging at 25 non-collinear diffusion gradient directions on a 3T MRI (GE medical system, Milwaukee, USA) with a matrix of 128×128, a voxel size of 1.96×1.96×2.6 mm^3, and a b-value of 1000 s/mm^2. The side of epileptogenicity was blinded during all lateralization processes. MTS was pathologically confirmed as Ammon's horn sclerosis by the pathologists in our institution.

Forty-eight subjects (23 females with age 33.2 ± 9.5, 25 males with age 31.2 ± 6.6) including twenty-five non-epileptic subjects recruited for a sleep research (numbered 1 to 25 in Table 2) and twenty-three healthy volunteers (numbered 25 to 48 in Table 2) were retrospectively included in this study as nonepileptic control subjects. They underwent the same 3.0T MRI system with the corresponding imaging sequences and imaging parameters. Forty-five subjects had T1-weighted images, twenty-five of which had FLAIR images and the other twenty had DWIs. The rest 3 subjects had only DWIs. Therefore, total of twenty-three subjects had DWIs (Table 2).

2.2. Image preprocessing

In order to perform an stable and smooth segmentation of the cingulum and fornix, the diffusion-weighted images were interpolated to produce a set of homogeneous voxels ($1.96\times1.96\times1.96$ mm^3) which were used to calculate diffusion tensor, FA, MD, and PDD (principal diffusion direction; eigenvector corresponding to the largest eigenvalue of the tensor).

2.3. Segmentation of the cingulum, fornix, and their subregions

Using previously described segmentation and fiber tracking methods [34], the cingulum and its subregions were bilaterally segmented for both datasets. In brief, the cingulum was segmented using an automatic seed-based algorithm: 1. A two-dimensional region of interest (ROI) was automatically extracted for each seed point. 2. Fiber tracking was performed between consecutive extracted ROIs. 3. The segmented cingulum was postprocessed through a morphological operation to achieve a connected and smoothed three-dimensional segmented structure. 4. The cingulum was finally divided into three subregions of posteroinferior, superior and anteroinferior for each left or right side using the points with highest curvature on the medial axis of the cingulum.

The fornix was also segmented using a previously described multiple ROIs fiber tracking method [34]. In brief, the fornix was segmented using a manual ROI-based algorithm: 1. Five ROIs were first manually depicted: A coronal ROI at the most anterior part of fornix body that is visible in a color-coded FA map. A coronal ROI at the branching point of fornix crura from the fornix body. A coronal ROI between the branching point and the most posterior part of fornix crura. An axial ROI at the most posterior part of fornix crura. An axial ROI at the most inferior part of fornix crura. 2. Fiber tracking was then performed between consecutive ROIs. 3. The fornix was finally divided into three subregions of body, left crus, and right crus using the branching point of the fornix crura from the fornix body.

2.4. Hippocampal T_1 volumetry, MD and FLAIR intensity analysis

The volumetrics of both left and right hippocampi from 20 TLE patients as well as 45 nonepileptic subjects were established from manually drawn ROIs. Using an affine registration tool (FLIRT; [35] T_1 images and the hippocampal boundaries were coregistered to MD and FLAIR images to acquire MD value and the mean and standard deviation of FLAIR intensity within the hippocampus [7, 9].

2.5. Group analysis of hemispheric variation of diffusion indices

The diffusion indices, FA and MD, were evaluated for any significant local variation throughout the cingulum across the nonepileptic subjects by comparing three cingulum subregions with the entire cingulum using t-test statistics. Moreover, the significance of the hemispheric variation of FA or MD within the cingulum subregions and the crus of fornix was tested in nonepileptic subjects using paired t-tests. Similarly, the significant of hemispheric variation of MD in the hippocampus was evaluated in nonepileptic subjects using paired t-tests.

For hippocampus, crus of fornix, and for any cingulum subregion where no significant hemispheric variation of FA or MD was observed in the nonepileptic subjects, two pairwise t-test statistical tests were performed: 1- The interhemispheric variation was determined on the sides ipsilateral and contralateral to the temporal epileptogenicity (the resected mesial temporal lobe) for the TLE and MTS cohorts 2- The TLE and MTS cohorts were compared with nonepileptic cohort to determine whether the TLE or MTS was in average associated with any significant bilateral variation. Any change with p-value less than 0.05 was considered statistically significant.

2.6. Individual analysis of hemispheric variation of an index

In order to determine whether an hemispheric variation of a measurable quantity in an individual patient is a true variation (beyond the uncertainty), it should compared with the HVU measured for that quantity in the specific region of interest. HVU can be estimated by asymmetry analysis of a cohort of nonepileptic subjects who have undergone imaging with the same scanner, under the same imaging conditions and segmentation method, for which no significant asymmetry is expected to be observed. An HVU was estimated for FA in the posteroinferior cingulum, FA in the crus of fornix, hippocampal volume, MD value, and the FLAIR signal intensities. For hippocampal volume and *mean* times *standard deviation* of the FLAIR intensity, the HVU was determined using the normalized measurements to their averages on both hippocampi. We then used the HVU levels to define the 95% confidence interval (CI) to distinguish true hemispheric variations for individual TLE and MTS patients.

2.7. HVU Estimation

Let I_{ik} be the observed value of an index I for the i^{th} subject (i = 1: n) in the k^{th} measurement (k = 1: K):

$$I_{ik}=\mu_i+\varepsilon_{ik} \quad (1)$$

which relates I_{ik} to its true value μ_i for each subject through a residual relative error ε_{ik} with the within-subject variance $\sigma_w^2=var(\varepsilon_{ik})$ in an ANOVA model [32, 33]. The within- and between-subject means of squares (WMS and BMS) with χ^2 distributions of *n(K-1)* and *n-1* degrees of freedom are calculated as:

$$WMS=\frac{1}{n(K-1)}\sum_{i=1}^{n}\sum_{k=1}^{K}[I_{ik}-\overline{I_{\text{ÉI}}}]^2 \quad (2)$$

and

$$BMS=\frac{k}{n}\sum_{i=1}^{n}[\overline{I_{\text{ÉI}}}-\bar{I}]^2 \quad (3)$$

respectively, where $\overline{I_{\text{ÉI}}}$ is the mean over all measurements for i^{th} subjects and $\bar{I}$ is the mean over all observations. As the measurements are acquired within hemispheric structures (K = 2), a within-subject standard deviation can be estimated by

$$\hat{\sigma_w} = \sqrt{WMS} = \sqrt{\frac{1}{2n}\sum_{i=1}^{n}[I_{ir} - I_{il}]^2} \quad (4)$$

where r and l denote right and left sides, respectively. The *HVU* is given by $2.77\sigma_w$ and is estimated by $2.77\sqrt{WMS}$. The hemispheric variation is expected to be in the range of –*HVU* to *HVU* for 95% of all nonepileptic subjects. Using a previously published formulation [32], the lower (HUV_L) and the upper (HVU_U) limits of the 95% confidence interval (CI) of the estimated *HVU* are calculated by:

$$HVU_L = 2.77\sqrt{\frac{n.WMS}{\chi^2_n(0.975)}}, HVU_U = 2.77\sqrt{\frac{n.WMS}{\chi^2_n(0.025)}} \quad (5)$$

For nonepileptic subjects, as both hemispheres undergo the same imaging condition and image processing course, any hemispheric variation may be attributable to natural physiological occurrences.

2.8. True individual hemispheric variation of an index

We supposed that for an index *I* in a given involved subregion of a TLE patient *i*, an hemispheric variation $\Delta I_i = I_{i,right} - I_{i,left}$ exists. A true individual hemispheric variation corresponds *to* $\mu_{i,right} - \mu_{i,left} \neq 0$, where μ is the index true value. Assuming $\varepsilon_{i,left}$ and $\varepsilon_{i,right}$ are independent and have the same within-subject standard deviation for all subjects, ΔI_i has a mean, $\mu_{i,right} - \mu_{i,left}$ and a within-subject variance, $2\sigma_w^2$. Therefore, the 95% CI for true hemispheric variation is $(\Delta I_i - 1.96\sqrt{2\sigma_w^2}\Delta I_i + 1.96\sqrt{2\sigma_w^2})$ or ($\Delta I_i - HVU$, $\Delta I_i + HVU$). If the 95% CI for $\mu_{i,contra} - \mu_{i,ipsi}$ does not contain zero and the true value of *HVU* is known, a 95% confidence exists of a true hemispheric variation for patient *i*. For taking into account the effect of a limited number of nonepileptic subjects on the degree of uncertainty around the estimate of *HVU*, an hemisphere variation is conservatively considered to be a true variation with 95% confidence if the interval ($\Delta I_i - HVU_U$, $\Delta I_i + HVU_U$) does not contain zero [32, 33].

3. Results

3.1. Group Analysis of Diffusion Hemispheric Variation

Figures 1A and 1B show a three-dimensional visualization of segmented cingulum and fornix and their subregions for a typical TLE patient.

In nonepileptic subjects, FA showed significant variation between the cingulum subregions ($p \leq 3.1 \times 10^{-5}$, Fig. 2). The superior subregion FA showed significant variability compared to its posteroinferior and anteroinferior neighbors ($p = 1.1 \times 10^{-11}$ and 1.2×10^{-6}, respectively). Significant variation of MD was not observed. Significant interhemispheric variations of the mean FA in nonepileptic subjects were observed (Fig. 2) for the entire cingulum ($p = 0.015$) and two of its subregions, the anteroinferior ($p = 0.024$) and the

superior (p = 0.00029), thereby making these regions poor candidates for tools for lateralization in patients with epilepsy.

No significant interhemispheric mean FA variation was observed in the posteroinferior subregion in the controls (left:right, 0.351:0.359; p = 0.42; Table 2; Fig. 2). However, both TLE and MTS cohorts showed a significant asymmetry in FA in ipsilateral side compared to contralateral side (ipsilateral:contralateral, 0.335:0.374, p= 0.025 ; ipsilateral:contralateral, 0.338:0.395, p=0.045 ; respectively; Fig 3). There was no significant bilateral variation observed in this subregion between TLE, MTS and nonepileptic cohorts (Fig 3).

No significant interhemispheric mean FA variation was observed in the crus of fornix in the controls (left:right, 0.364:0.359; p = 0.55; Table 2; Fig. 4). However, both TLE and MTS cohorts showed a significant asymmetry in FA in ipsilateral crus compared to contralateral crus (ipsilateral:contralateral, 0.308:0.338, p=0.031 ; ipsilateral:contralateral, 0.310:0.356, p=0.023, respectively; Fig 4). A significant bilateral variation was also observed in the fornix crus in TLE and MTS cohorts compared to nonepileptic cohorts (p= 0.002, p=0.04, respectively; Fig 4).

No significant interhemispheric MD variation was observed in nonepileptic cohort (left: right, 0.00105: 0.00104, p = 0.59; Table 2; Fig. 5). However, a significant interhemispheric MD variation was observed in both TLE and MTS cohorts (ipsilateral: contralateral, 0.00129: 0.00109, p = 0.000036; ipsilateral: contralateral, 0.00132: 0.00107, p = 0.00021; respectively; Fig. 5). Both TLE and MTS cohorts showed a significant bilateral variation in MD in hippocampus compared to the nonepileptic cohort ($p = 3 \times 10^{-6}$, $p = 7 \times 10^{-6}$, respectively; Fig 5).

These finding suggest that FA in posterior cingulum and crus of fornix, as well as MD in hippocampus could act as potential biomarkers to lateralize the epileptogenic temporal lobe.

3.2. Individual analysis of hemispheric variation for FA in posteroinferior cingulum and fornix crus, volumetric, MD value, and FLAIR intensity in hippocampus

Using nonepileptic subjects, the *HVU* and its 95% CI (HVU_L, HVU_U) were estimated and listed in Table 3.

For each individual of the cohorts of TLE and MTS patients, a determination was made as to whether a hemispheric variation of mentioned biomarkers was beyond uncertainty (Table 4; Fig 6). For all MTS cases, the posteroinferior cingulum and the fornix crus had a lower FA, and the hippocampus had a smaller volume, higher MD value and higher FLAIR intensity on the side of the patient's epileptogenicity. However, the hemispheric variation of hippocampal volume and FA in fornix crus was within the uncertainty for one pathology-proven MTS case. The hemispheric variation of FA in the posteroinferior cingulum, FA in the fornix crus, the hippocampal MD value, FLAIR intensity, and the volume were beyond the uncertainty for 15, 14, 18, 13, and 16 TLE patients respectively and lateralized them. While the FA in posteroinferior cingulum, hippocampal MD and hippocampal volumetry did not have any false-positives in lateralization of TLE, the lateralization results for the

hippocampal FLAIR intensity and FA in fornix crus analysis were wrong for two non-MTS TLE cases.

Consolidating lateralization results of HVU analysis on all mentioned biomarkers by majority voting detected the epileptogenic side for 19 out of 20 TLE cases with no wrong lateralization (Table 4).

4. Discussion

Quantitative neuroimaging biomarkers are increasingly used as means of lateralizing temporal lobe epilepsy in attempts to lessen diagnostic ambiguity and avoid invasive electrographic monitoring approaches. The present findings of an elevated mean diffusivity in the hippocampus and reduced fractional anisotropy in the posteroinferior cingulum and fornix crus ipsilateral to the side of mesial temporal epileptogenicity align well with the known attributes of a reduced hippocampal volume and corresponding elevated FLAIR MR signal intensity in indicating laterality in mTLE. Moreover, an assessment of interhemispheric variation, applied here to these related limbic structures, is a necessary component in the analysis of imaging attributes to ensure the certainty of a true difference in the individual patient. The introduction of the HVU as a metric in this study provides the means to establish the trueness in outcome for all measures. In turn, this allows comparison of imaging attributes in order to better judge their relative efficacy in lateralizing the ictal onset zone in TLE.

The presence of variability in a quantitative imaging index can be due to the imaging system-related or subject-related factors, which make a variation in an index measured in an individual patient difficult to interpret. However, in hemispherical asymmetry analysis, since the paired bilateral structures undergo the same imaging condition, the variability in the extracted interhemispheric index could be confined to the subject-related factors including natural physiological occurrences and pathology. In the current study, in order to determine whether the variation can quite purely account for the pathology, the variability for natural physiological occurrences was estimated from a cohort of control, nonepileptic subjects who had undergone imaging with the same scanner and imaging parameters. Subsequently, if the observed interhemispheric variation for an individual patient was beyond the natural physiological occurrences (uncertainty), a true -significant pathology-induced variation was determined by a conservative rigor of applying an upper and lower limit of a 95% confidence interval.

Extensive changes have been identified in the hippocampus and limbic network at large in cases of mTLE associated with hippocampal sclerosis using diffusion tensor imaging and voxel-based methods [29, 30]. Elevation of ipsilateral hippocampal MD was accompanied by a disparity in the extent of FA change in the limbic system. More widespread reduction was evident with left mTLE than right mTLE [30]. Others have reported changes in tract integrity in the corpus callosum, fornix and cingulum [16–18, 20–24]. The cingulum was shown to have overall high diffusivity in cases of mTLE, with or without MTS, although FA was reduced in only the nonlesional cases. Our observation indicated that FA in posteroinferior cingulum and fornix crus, as well as MD in hippocampus would be accurate

imaging biomarkers for MTS and strong indicators of laterality in TLE patients, including those without pathologically-proven hippocampal sclerosis. Notably, five of the 20 patients found to be without hippocampal sclerosis but with gliosis were, in fact, identified with MTS preoperatively and were accurately denoted by these markers. We also observed both TLE and MTS were associated with significant bilateral variation of FA in the fornix crus and MD in the hippocampus, compared with the nonepileptic control cohort, which was in agreement with the previous studies [18, 23, 24]. However, we did not observe significant bilateral changes in FA and MD either in the cingulum or its subregions, compared with the nonepileptic control cohort, in contrast with previous reports [17, 18, 24].

Hemispheric specialization ostensibly influences fiber tract projections and branch patterns in superior and anteroinferior subregions to a sufficient degree to be distinguishable, whereas, it would not appear to be a factor in the posteroinferior subregion in nonepileptic subjects. The reduction in anisotropy in this subregion ipsilateral to a TLE would suggest the loss of a predominant directionality of fibers as a consequence of demyelination or axonal degradation.

The anterior and posterior descending segments of the cingulum are difficult to delineate without adequately defined regions-of-interest (ROIs) [17, 18, 36]. The seed-based segmentation-tractography method overcomes this limitation and is more suited to assessing thickness, particularly, in both the anterior and posterior descending segments [34]. Normalization was not applied to the diffusion-based hemispheric variation methods because FA and MD values are region-specific meaningful information which should be preserved to be able to differentiate between estimates of uncertainty in different fiber tracts or brain regions. Moreover, the proposed method of assessing true variation in FA better preserved information content as the diffusion tensor imaging data was processed without applying coregistration or smoothing.

Comparison of a diffusion index in paired structures with an index mean established in a control group can be misleading when bilateral changes are noted as these may be a consequence of spurious physiological change rather than a marker of epileptogenicity. The variability of an extracted index has been addressed comprehensively in several studies by repeated (i.e., test-retest) measurements [33, 37–41]. The choice of a subregion of the cingulum where there is little variability in controls and the implementation of the HVU analysis neutralizes the issues of scanner choice and imaging parameters while avoiding the need for coregistration. It is, therefore, restricted to subject-specific and fiber-specific features (i.e., fiber tract size, shape and diffusivity pattern) of the image and, ostensibly, reduces the uncertainty in declaring true FA and MD variation.

Atrophy of the cingulum has been found to be a common feature in left mesial TLE, whether associated with hippocampal sclerosis or in cryptogenic cases wherein no distinct MR imaging characteristics may be identified [42]. Voxel-based morphometry measures of both right and left cingula identified reductions of gray matter volumes in cases of left mTLE along with similar changes in the left parahippocampal and superior temporal gyri, the frontal regions and the cerebellum. Hemispheric variation uncertainty was not applied in this study to establish the robustness of these regional distinctions in order to establish laterality.

The precision of hippocampal segmentation is an important factor in the analysis of not only volume but of FLAIR intensity and MD. Both the accuracy of border delineation and reproducibility influence case-specific interhemispheric and cohort comparisons. Performance of automatic segmentation methods varies across subjects and may not be as reliable as supervised segmentation of the hippocampus in providing greater assurance of uniformity, although even entirely manual delineation is subject to reproducibility error; moreover, it is time-consuming, amounting to upwards of five hours with cranial stripping. In the case of MD and FLAIR analysis, the necessary coregistration of image domains may further compromise accuracy and contaminate results. Such arguments support a preference for the application of FA in the posteroinferior cingulum and fornix crus rather than the hippocampus, despite the strong performance of hippocampal MD as a lateralizing asset for TLE. The greatly reduced processing time, averaging only 30 minutes including tensor analysis, and the improved anatomical accuracy of a supervised seed insertion in the cingulum provides the confidence to establish a more definitive result in the case of FA.

As we included small-sized cohorts for TLE, MTS, and nonepileptic control, the results of group analyses should be considered with caution. Sensitivity of individual analysis of hemispheric variation depends on the number of control subjects, since recruiting more control subjects will lead to a more accurate estimation of HVU with a narrower confidence interval. As the number of subjects approaches infinity, the estimated HVU and the upper and lower limits of its confidence interval approach the true HVU ($\hat{HVU}$, HVU_L, $HVU_U \rightarrow HVU$). However, a medium-sized control cohort would still be adequate to estimate a sufficiently accurate HVU with a sufficiently narrow CI to detect subtle individual hemispheric variations. Another limitation of the study is how to integrate various lateralization results in the process of detecting the epileptogenic side. Although consolidating lateralization results of HVU analysis by simple majority voting, detected the epileptogenic side for 19 of 20 TLE cases with no wrong lateralization, still weighted integration of lateralization results of various imaging biomarkers may outperform majority voting and should be further studied.

The use of HVU analysis with more precise structural distinction of paired anatomical sites promises to provide greater confidence in surgical decision-making and, in some cases, will obviate the need for extraoperative ECoG in cases for which lateralization of TLE is unclear. Prospective studies with these applications will settle the matter.

5. Conclusions

Hemispheric variation analysis in individual mTLE patients was applied to hippocampal volumetry and FLAIR signal intensity and to the newly proposed biomarkers, fractional anisotropy of the posteroinferior subregion of the cingulum and crus of fornix and mean diffusivity in the hippocampus. These measures could correctly lateralize mTLE in patients who underwent surgery with Engel class I outcomes, even in those for whom extraoperative ECoG was felt to be necessary. This study supports the notion that HVU analysis has a role as an application to a battery of quantitative imaging studies that, in concert, may be used to support clinical decision-making in the evaluation of TLE.

Acknowledgments

Special thanks to Abdelrahman Hassane, Oltion Meci, Harrini Vijay, and Mohammad Emari for their invaluable helps in data processing.

Funding statement

This work was supported in part by NIH grant R01EB013227.

References

1. Engel J Jr. Surgery for seizures. New England Journal of Medicine. 1996; 334(10):647–653. [PubMed: 8592530]
2. Achten E, et al. Value of single-voxel proton MR spectroscopy in temporal lobe epilepsy. American journal of neuroradiology. 1997; 18(6):1131–1139. [PubMed: 9194441]
3. Vainio P, et al. Reduced N-acetylaspartate concentration in the temporal lobe epilepsy by quantitative 1H MRS in vivo. NeuroReport-International Journal for Rapid Communications of Research in Neuroscience. 1994; 5(14):1733–1736.
4. de Tisi J, et al. The long-term outcome of adult epilepsy surgery, patterns of seizure remission, and relapse: a cohort study. The Lancet. 2011; 378(9800):1388–1395.
5. Jack CR Jr, et al. Magnetic resonance image–based hippocampal volumentry: Correlation with outcome after temporal lobectomy. Annals of neurology. 1992; 31(2):138–146. [PubMed: 1575452]
6. Jackson G, et al. Optimizing the diagnosis of hippocampal sclerosis using MR imaging. American journal of neuroradiology. 1993; 14(3):753–762. [PubMed: 8517369]
7. Jafari-Khouzani K, et al. FLAIR signal and texture analysis for lateralizing mesial temporal lobe epilepsy. Neuroimage. 2010; 49(2):1559–1571. [PubMed: 19744564]
8. Lopez-Acevedo ML, et al. Secondary MRI-findings, volumetric and spectroscopic measurements in mesial temporal sclerosis. Swiss Med Wkly. 2012; 142:w13549. [PubMed: 22688826]
9. Akhondi-Asl A, et al. Hippocampal volumetry for lateralization of temporal lobe epilepsy: automated versus manual methods. Neuroimage. 2011; 54:S218–S226. [PubMed: 20353827]
10. Baulac M, et al. Correlations Between Magnetic Resonance Imaging-Based Hippocampal Sclerosis and Depth Electrode Investigation in Epilepsy of the Mesiotemporal Lobe. Epilepsia. 1994; 35(5): 1045–1053. [PubMed: 7925150]
11. Schiller Y, Cascino GD, Sharbrough FW. Chronic intracranial EEG monitoring for localizing the epileptogenic zone: an electroclinical correlation. Epilepsia. 1998; 39(12):1302–1308. [PubMed: 9860065]
12. Bulacio JC, et al. Long-term seizure outcome after resective surgery in patients evaluated with intracranial electrodes. Epilepsia. 2012; 53(10):1722–1730. [PubMed: 22905787]
13. Arya R, et al. Adverse events related to extraoperative invasive EEG monitoring with subdural grid electrodes: A systematic review and meta-analysis. Epilepsia. 2013
14. Kuzniecky R, et al. Multimodality MRI in mesial temporal sclerosis: relative sensitivity and specificity. Neurology. 1997; 49(3):774–778. [PubMed: 9305339]
15. Pierpaoli C, et al. Water diffusion changes in Wallerian degeneration and their dependence on white matter architecture. Neuroimage. 2001; 13(6):1174–1185. [PubMed: 11352623]
16. Rugg-Gunn F, et al. Diffusion tensor imaging of cryptogenic and acquired partial epilepsies. Brain. 2001; 124(3):627–636. [PubMed: 11222461]
17. Liacu D, et al. Diffusion tensor imaging tractography parameters of limbic system bundles in temporal lobe epilepsy patients. Journal of Magnetic Resonance Imaging. 2012
18. Concha L, Beaulieu C, Gross DW. Bilateral limbic diffusion abnormalities in unilateral temporal lobe epilepsy. Annals of neurology. 2004; 57(2):188–196. [PubMed: 15562425]
19. Kim CH, et al. Thalamic changes in temporal lobe epilepsy with and without hippocampal sclerosis: a diffusion tensor imaging study. Epilepsy research. 2010; 90(1–2):21. [PubMed: 20307957]

20. Yogarajah M, Duncan JS. Diffusion-based magnetic resonance imaging and tractography in epilepsy. Epilepsia. 2008; 49(2):189–200. [PubMed: 17941849]
21. Gross DW, Concha L, Beaulieu C. Extratemporal white matter abnormalities in mesial temporal lobe epilepsy demonstrated with diffusion tensor imaging. Epilepsia. 2006; 47(8):1360–1363. [PubMed: 16922882]
22. Kim H, et al. Secondary white matter degeneration of the corpus callosum in patients with intractable temporal lobe epilepsy: a diffusion tensor imaging study. Epilepsy research. 2008; 81(2–3):136–142. [PubMed: 18572387]
23. Concha L, et al. In vivo diffusion tensor imaging and histopathology of the fimbria-fornix in temporal lobe epilepsy. The Journal of Neuroscience. 2010; 30(3):996–1002. [PubMed: 20089908]
24. Concha L, et al. White-matter diffusion abnormalities in temporal-lobe epilepsy with and without mesial temporal sclerosis. Journal of Neurology, Neurosurgery & Psychiatry. 2009; 80(3):312–319.
25. Thivard L, et al. Diffusion tensor imaging in medial temporal lobe epilepsy with hippocampal sclerosis. Neuroimage. 2005; 28(3):682–690. [PubMed: 16084113]
26. Hugg JW, Butterworth EJ, Kuzniecky RI. Diffusion mapping applied to mesial temporal lobe epilepsy Preliminary observations. Neurology. 1999; 53(1):173–173. [PubMed: 10408555]
27. Wieshmann UC, et al. Water diffusion in the human hippocampus in epilepsy. Magnetic resonance imaging. 1999; 17(1):29–36. [PubMed: 9888396]
28. Ahmadi ME, et al. Side matters: diffusion tensor imaging tractography in left and right temporal lobe epilepsy. American journal of neuroradiology. 2009; 30(9):1740–1747. [PubMed: 19509072]
29. Yoo SY, et al. Apparent diffusion coefficient value of the hippocampus in patients with hippocampal sclerosis and in healthy volunteers. American journal of neuroradiology. 2002; 23(5): 809–812. [PubMed: 12006282]
30. Focke NK, et al. Voxel-based diffusion tensor imaging in patients with mesial temporal lobe epilepsy and hippocampal sclerosis. Neuroimage. 2008; 40(2):728–737. [PubMed: 18261930]
31. Labate A, et al. Hippocampal and thalamic atrophy in mild temporal lobe epilepsy A VBM study. Neurology. 2008; 71(14):1094–1101. [PubMed: 18824674]
32. Barnhart HX, Barboriak DP. Applications of the repeatability of quantitative imaging biomarkers: a review of statistical analysis of repeat data sets. Translational oncology. 2009; 2(4):231–235. [PubMed: 19956383]
33. Nazem-Zadeh M-R, et al. Uncertainty in assessment of radiation-induced diffusion index changes in individual patients. Physics in medicine and biology. 2013; 58(12):4277–4296. [PubMed: 23732399]
34. Nazem-Zadeh MR, et al. Radiation therapy effects on white matter fiber tracts of the limbic circuit. Medical physics. 2012; 39(9):5603–5613. [PubMed: 22957626]
35. Jenkinson M, et al. Improved optimization for the robust and accurate linear registration and motion correction of brain images. Neuroimage. 2002; 17(2):825–841. [PubMed: 12377157]
36. Wakana S, et al. Reproducibility of quantitative tractography methods applied to cerebral white matter. Neuroimage. 2007; 36(3):630–644. [PubMed: 17481925]
37. Cutajar M, et al. Test-retest reliability and repeatability of renal diffusion tensor MRI in healthy subjects. European journal of radiology. 2011; 80(3):e263–e268. [PubMed: 21227619]
38. Froeling M, et al. Reproducibility of diffusion tensor imaging in human forearm muscles at 3.0 T in a clinical setting. Magnetic Resonance in Medicine. 2010; 64(4):1182–1190. [PubMed: 20725932]
39. Beattie PF, Morgan PS, Peters D. Diffusion-weighted magnetic resonance imaging of normal and degenerative lumbar intervertebral discs: a new method to potentially quantify the physiologic effect of physical therapy intervention. The Journal of orthopaedic and sports physical therapy. 2008; 38(2):42–49. [PubMed: 18560192]
40. Cercignani M, et al. Inter-sequence and inter-imaging unit variability of diffusion tensor MR imaging histogram-derived metrics of the brain in healthy volunteers. American journal of neuroradiology. 2003; 24(4):638–643. [PubMed: 12695195]

41. Paldino MJ, et al. Repeatability of quantitative parameters derived from diffusion tensor imaging in patients with glioblastoma multiforme. Journal of Magnetic Resonance Imaging. 2009; 29(5): 1199–1205. [PubMed: 19388113]

42. Riederer F, et al. Network atrophy in temporal lobe epilepsy A voxel-based morphometry study. Neurology. 2008; 71(6):419–425. [PubMed: 18678824]

Highlights

- Introduction of epileptogenicity biomarkers based on diffusion tensor imaging
- Estimation hemispheric variation uncertainty for hippocampus and cingulum indices
- Confirmation of laterality of epileptogenicity in mesial temporal sclerosis patients
- Enhancement of confidence of clinical decision-making regarding surgical candidacy
- Reduction of the need for implantation of intracranial monitoring electrodes

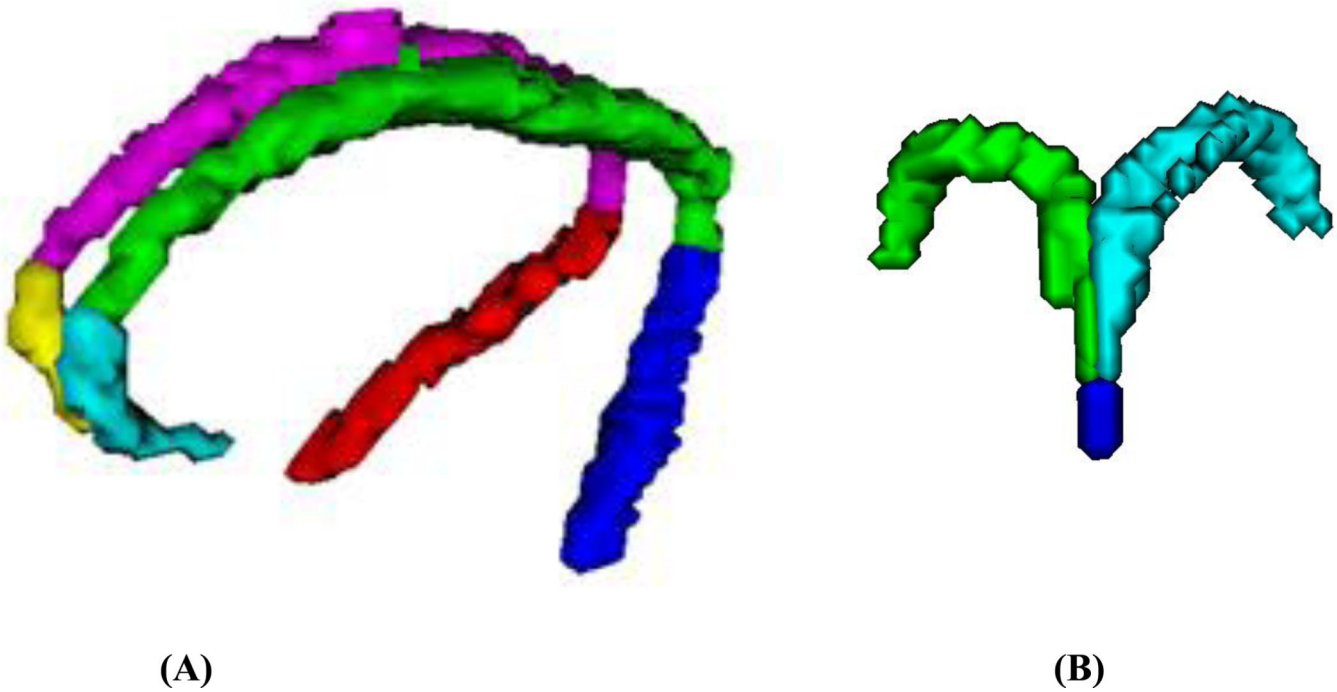

Figure 1. Segmentation of cingulum and fornix and their subregions

(A): Three dimensional visualization of the segmented cingulum subregions of posteroinferior right (red) and left (blue), superior right (magenta) and left (green), and the anteroinferior right (yellow) and left (cyan).

(B): Three dimensional visualization of the segmented fornix subregions of body (blue), right crus (green) and left crus (cyan) for the same patient.

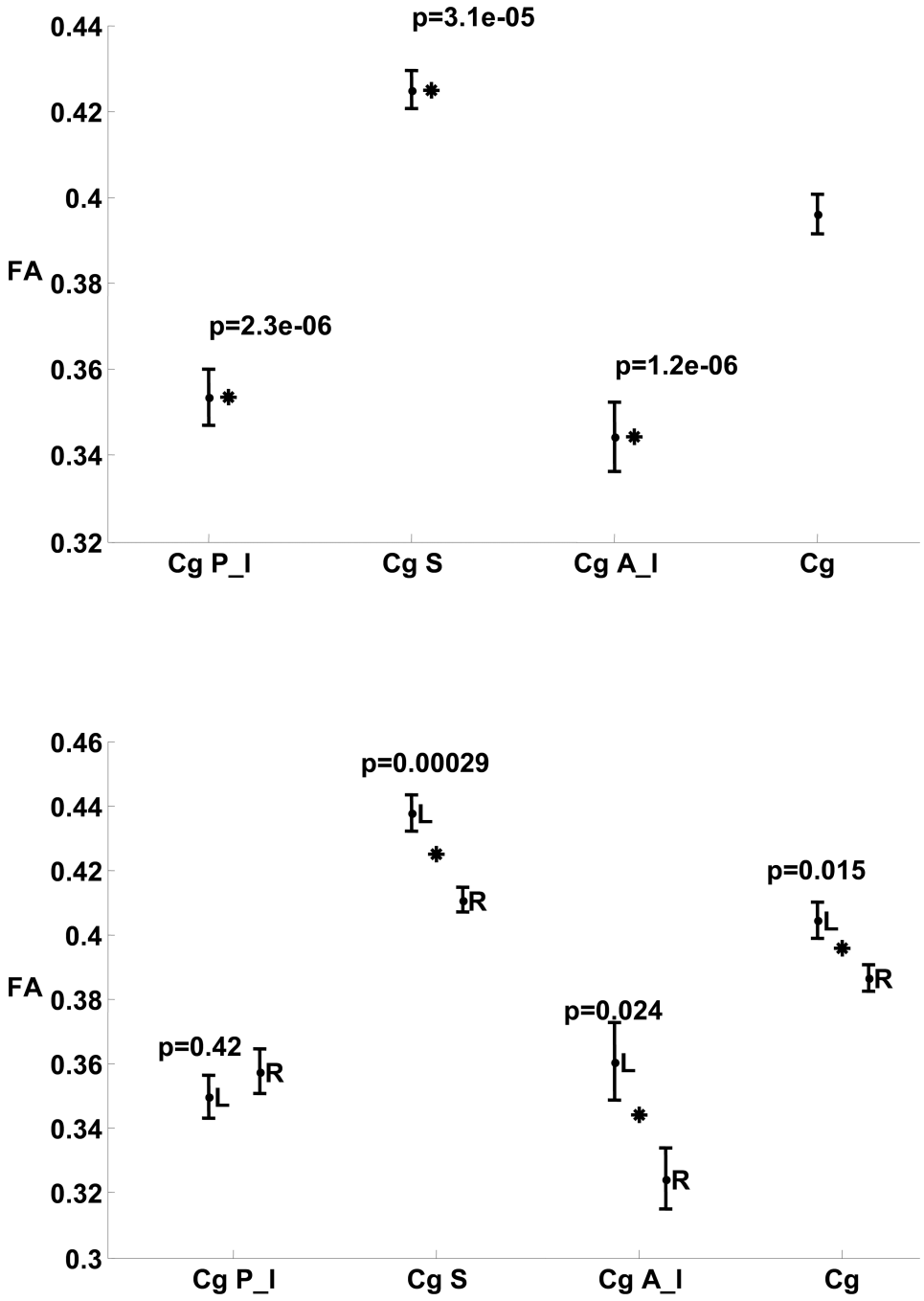

Figure 2. Comparing FA in cingulum subregions of nonepileptic subjects

Top: P-values are for comparison of FA in individual cingulum subregions with cingulum overall.

Bottom: P-values are for comparison of FA in left and right hemispheres of cingulum overall and its subregions.

Stars indicate statistical significance.

Figure notation: FA, fractional anisotropy; Cg, cingulum overall; P_I, posteroinferior; S, superior; A_I, anteroinferior; L, left, R, right.

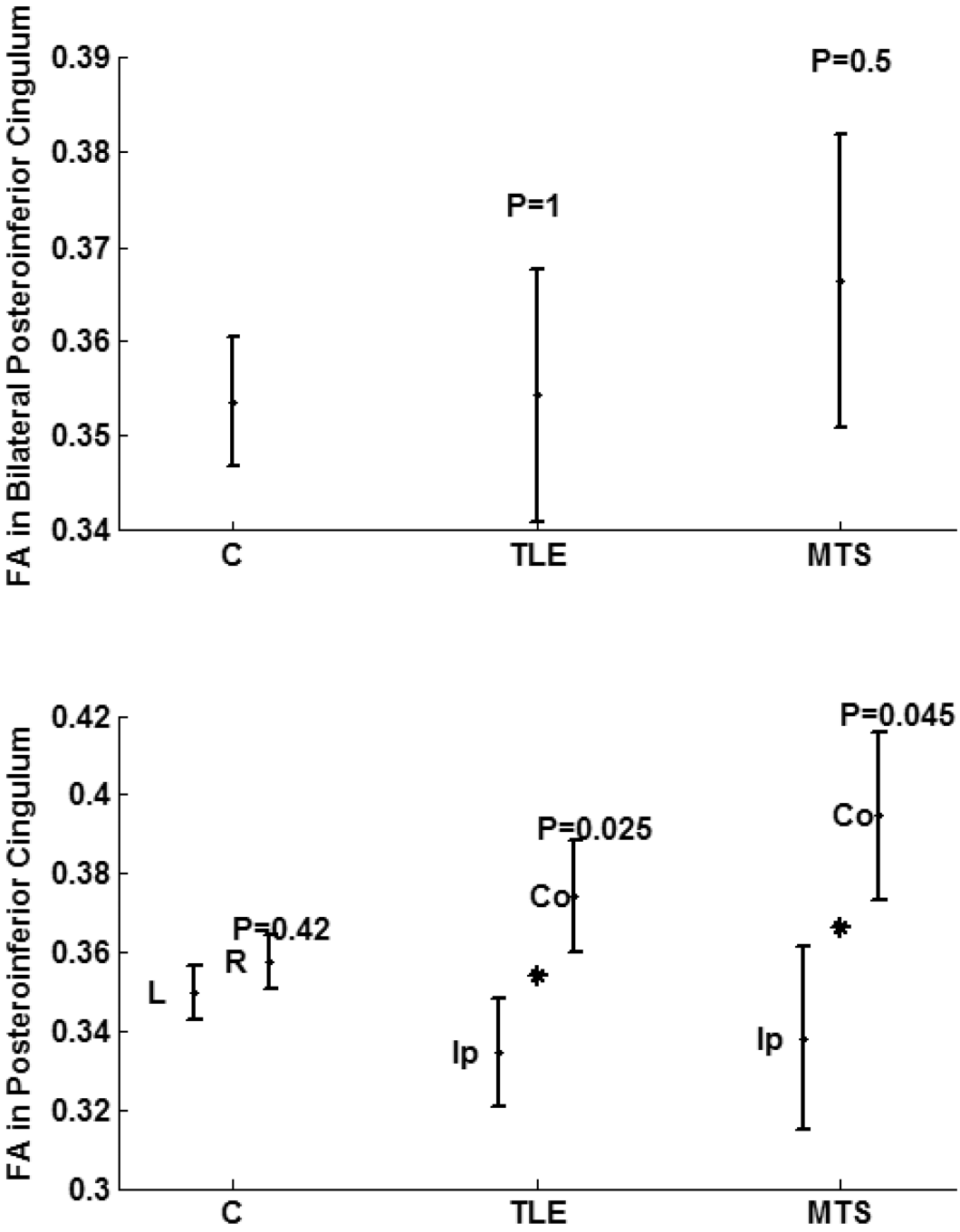

Figure 3. Comparing FA in posteroinferior cingulum of cohorts of nonepileptic subjects, TLE patients, and the subset of TLE patients with pathology proven MTS

Top: Bilateral variations. Bottom: Hemispheric variation between left and right hemispheres for nonepileptic subjects, and between structures ipsilateral and contralateral sides to the epileptogenicity. Stars indicate statistical significance and P indicate the significance p-value.

Figure notation: FA, fractional anisotropy; L, left, R, right; Ip, ipsilateral; Co, contralateral.

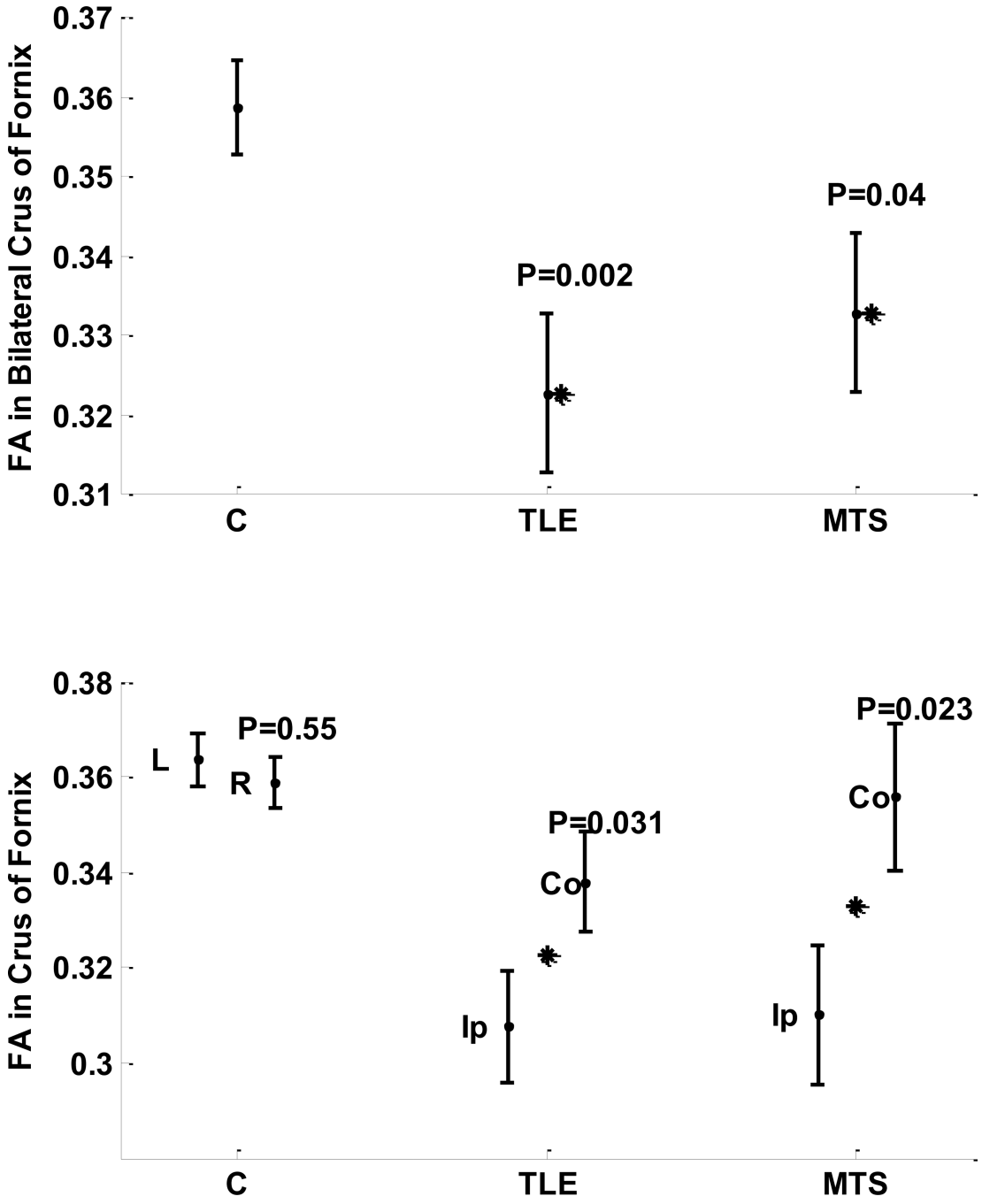

Figure 4. Comparing FA in fornix crus of cohorts of nonepileptic subjects, TLE patients, and the subset of TLE patients with pathology proven MTS

Top: Bilateral variations. Bottom: Hemispheric variation between left and right hemispheres for nonepileptic subjects, and between structures ipsilateral and contralateral sides to the epileptogenicity. Stars indicate statistical significance and P indicate the significance p-value.

Figure notation: FA, fractional anisotropy; L, left, R, right; Ip, ipsilateral; Co, contralateral.

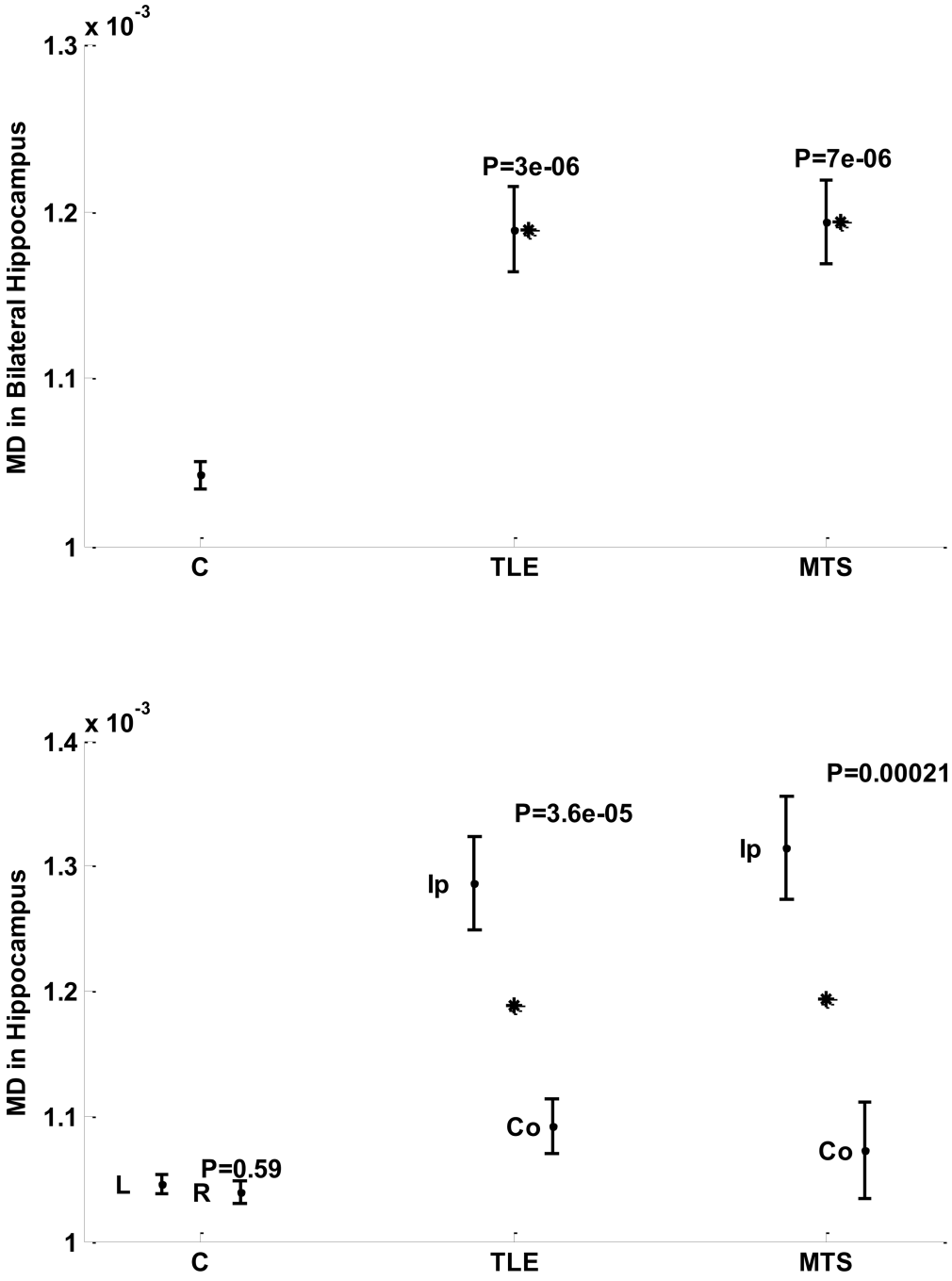

Figure 5. Comparing MD in hippocampus of cohorts of nonepileptic subjects, TLE patients, and the subset of TLE patients with MTS

Top: Bilateral variations. Bottom: Hemispheric variation between left and right hemispheres for nonepileptic subjects, and between structures ipsilateral and contralateral sides to the epileptogenicity.

Stars indicate statistical significance and P indicate the significance p-value.

Figure notation: MD, mean diffusivity; L, left, R, right; Ip, ipsilateral; Co, contralateral.

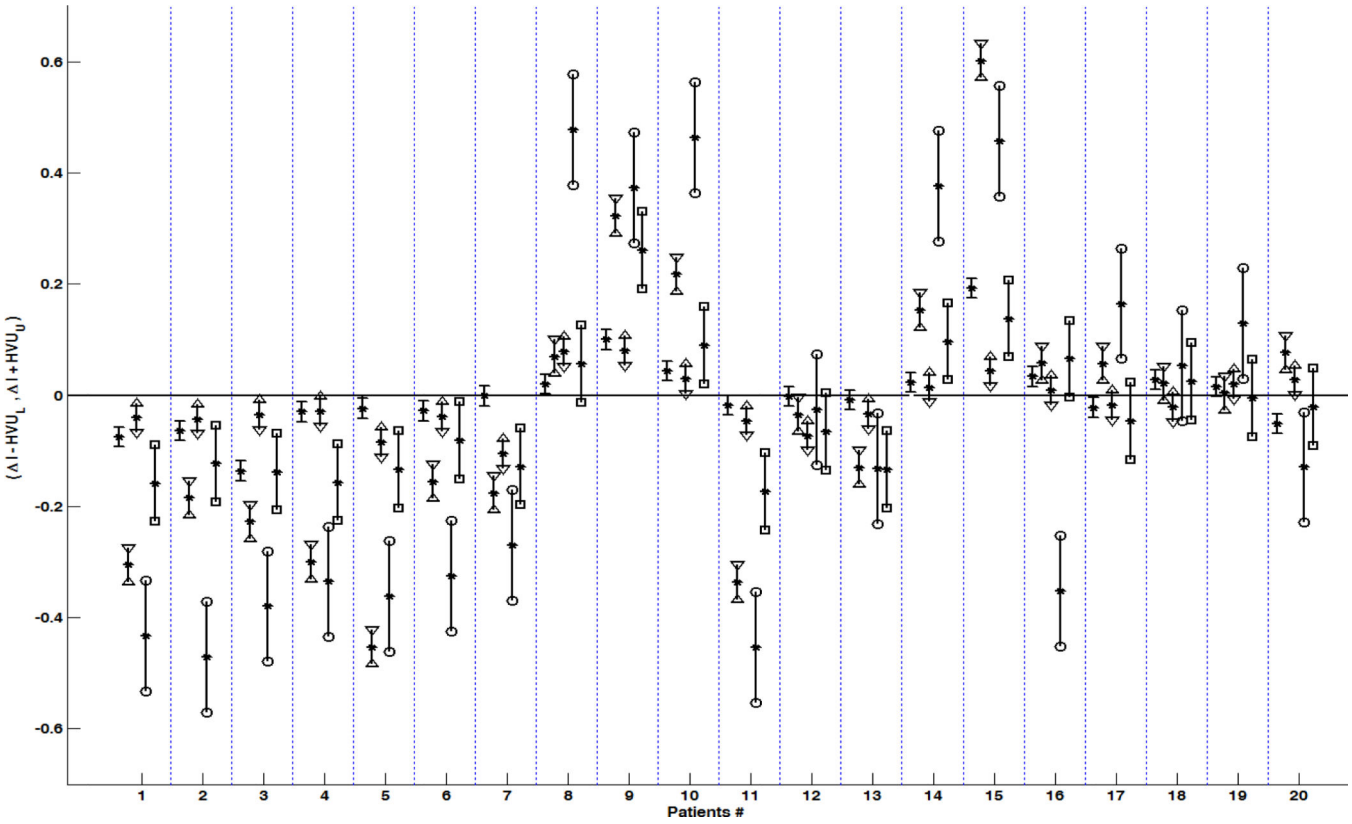

Figure 6. The 95% confidence interval (CI) of true hemispheric variations for individual TLE patients

Suppose that μ_{ipsi} and μ_{contra} are true value of index *I* in ipsilateral and contralateral sides to epileptogenicity and $\Delta I = I_{right} - I_{left}$ is the hemispheric variation (depicted by stars). The 95% CI of $\mu_{contra} - \mu_{ipsi}$ was calculated as ($\Delta I - HVU_U$, $\Delta I + HVU_U$) for ΔI as the hemispheric variation of FA within the fornix crus (depicted between minuses), FA within the posteroinferior cingulum (depicted between triangles facing inward), the hemispheric variation of hippocampal MD (triangles facing outward), the hemispheric variation for hippocampal volumetrics (between squares), and the hemispheric variation for hippocampal FLAIR signal intensities (between circles). An individual patient was considered to have a true hemispheric variation if the 95% CI of the true hemispheric variation did not contain zero.

Note that the Patients# 1 to 10 belong to TLE patients with pathology proven MTS.

J Neurol Sci. Author manuscript; available in PMC 2015 July 15.

Table 1

Patient characteristics.

No	TLE Duration (years)	Pathologically proven MTS	Pathology	Side	Risk Factor	ECoG	Reason for ECoG	Age at Surgery (years)	Follow-up Duration (years)
1	35	Y	AHS	L	closed head injury	Y	temporal vs. extratemporal	53.6	2.8
2	59	Y	AHS	L	febrile seizure (18 months), minor closed head injury	N		61	4.5
3	5	Y	AHS	L	febrile seizure, heroin abuse with multiple overdoses	Y	R vs L	45.8	2.5
4	39	Y	AHS	L	febrile seizure	N		43.9	2.6
5	59	Y	AHS	L	febrile seizure	N		60.7	4.3
6	31	Y	AHS	L	closed head injury; fever	N		51.6	4.4
7	18	Y	AHS	L	meningitis (18 months)	N		38.4	2.9
8	10	Y	AHS	R	febrile seizure	Y	R vs. L	15.0	4.6
9	47	Y	AHS	R	Fetal ethyl alcohol syndrome	Y	temporal vs. extratemporal	47.5	5.3
10	28	Y	CA, AHS	R	None	N		49.0	4.0
11	28	N	nonspecific CA (Corpora amylacea) no pathology on hippocamp	L	febrile seizure (24 months)	N		30.4	3.2
12	37	N	No specimen received	L	febrile seizure	N		39.3	2.6
13	27	N	FCD	L	None	N		28.7	2.6
14	12	N	Non-diagnostic specimen (too small)	R	closed head injury	N		27.3	3.7
15	47	N	gliosis, FCD	R	febrile seizure, cerebral palsy	N		48.3	4.0
16	6	N	nonspecific changes	R	childhood sz related to fluid management after intussusceptions	N		28.6	4.2
17	46	N	ill-defined hippocampal structure with suggestion of mild neuronal loss	R	childhood meningitis	Y	R vs. L temporal vs. extratemporal	53.1	4.3
18	8	N	No hippocampus received	R	closed head injury	Y	R vs. L	43.7	3.5
19	8	N	—	R	closed head injury	N		27.7	5.4
20	29	N	temporal pole granulomas	R	physical abuse	Y	temporal vs. extratemporal	45.1	4.1

Table notation: ECoG, electrocorticography; TLE, temporal lobe epilepsy; L, left; R, right; CA, corpora amylacea; AHS, Ammon's horn sclerosis; FCD, focal cortical dysplasia; Y, Yes; N, No.

J Neurol Sci. Author manuscript; available in PMC 2015 July 15.

Table 2

Volumetry, FLAIR signal intensity analysis, and MD Value analysis for left and right hippocampi, and FA value analysis for left and right posteroinferior cingulum in 48 nonepileptic subjects.

Control No	Hippocampal Volumetrics		Hippocampal FLAIR Intensity (Mean±StD)		Posteroinferior Cingulum FA		Fornix Crus FA		Hippocampal MD value	
	Left	Right	Left	Right	Left	Right	Left	Right	Left	Right
1	3135.2	2926.6	215.2±27.2	212.4±30.4	NA	NA	NA	NA	NA	NA
2	2406.9	2525.2	221.7±26.4	222.2±28.5	NA	NA	NA	NA	NA	NA
3	2450.8	2427.6	233.8±24.0	231.7±29.3	NA	NA	NA	NA	NA	NA
4	2761.9	2833.9	202.7±25.7	206.4±26.1	NA	NA	NA	NA	NA	NA
5	2278.8	2184.9	257.2±24.9	259.2±25.7	NA	NA	NA	NA	NA	NA
6	3404.8	3453.6	238.3±22.3	237.3±25.9	NA	NA	NA	NA	NA	NA
7	2541.1	2428.9	176.9±38.8	177.8±37.3	NA	NA	NA	NA	NA	NA
8	2783.9	2912.0	241.5±25.8	242.9±27.9	NA	NA	NA	NA	NA	NA
9	2181.2	2461.8	271.1±27.7	261.1±28.8	NA	NA	NA	NA	NA	NA
10	2476.4	2115.3	262.1±30.6	266.1±30.2	NA	NA	NA	NA	NA	NA
11	2494.7	2774.1	269.7±27.1	271.2±29.2	NA	NA	NA	NA	NA	NA
12	2885.1	2851.0	257.9±28.9	259.1±29.2	NA	NA	NA	NA	NA	NA
13	2402.0	2189.8	238.2±25.2	237.6±27.0	NA	NA	NA	NA	NA	NA
14	2324.0	2400.8	236.5±28.5	234.4±31.2	NA	NA	NA	NA	NA	NA
15	2210.5	2414.2	273.0±26.3	271.2±24.4	NA	NA	NA	NA	NA	NA
16	2100.7	2287.4	207.3±24.5	210.2±25.5	NA	NA	NA	NA	NA	NA
17	2040.9	2069.0	219.5±25.9	221.6±26.8	NA	NA	NA	NA	NA	NA
18	2781.4	2585.0	203.8±26.5	211.4±26.3	NA	NA	NA	NA	NA	NA
19	2270.3	2366.6	213.5±25.9	211.4±28.0	NA	NA	NA	NA	NA	NA
20	2833.9	2782.6	207.2±20.6	210.9±23.9	NA	NA	NA	NA	NA	NA
21	2469.1	2324.0	242.6±27.1	245.3±30.0	NA	NA	NA	NA	NA	NA
22	2505.7	2587.5	262.5±33.4	257.7±37.3	NA	NA	NA	NA	NA	NA
23	2703.3	2658.2	185.1±28.6	193.7±29.0	NA	NA	NA	NA	NA	NA
24	2521.6	2393.5	258.4±30.5	260.1±28.7	NA	NA	NA	NA	NA	NA

J Neurol Sci. Author manuscript; available in PMC 2015 July 15.

Control No	Hippocampal Volumetrics		Hippocampal FLAIR Intensity (Mean±StD)		Posteroinferior Cingulum FA		Fornix Crus FA		Hippocampal MD value	
	Left	Right	Left	Right	Left	Right	Left	Right	Left	Right
25	2051.3	2244.6	212.1±24.0	212.2±26.2	NA	NA	NA	NA	NA	NA
26	NA	NA	NA	NA	0.328	0.369	0.378	0.377	NA	NA
27	NA	NA	NA	NA	0.430	0.424	0.397	0.386	NA	NA
28	NA	NA	NA	NA	0.379	0.353	0.379	0.373	NA	NA
29	17950.0	18875.0	NA	NA	0.411	0.461	0.453	0.432	0.00109	0.00110
30	14708.0	15547.0	NA	NA	0.302	0.325	0.361	0.345	0.00106	0.00103
31	15284.0	16241.0	NA	NA	0.322	0.312	0.363	0.339	0.00102	0.00105
32	14632.0	16210.0	NA	NA	0.359	0.364	0.364	0.373	0.00105	0.00107
33	17678.0	18195.0	NA	NA	0.371	0.363	0.358	0.371	0.00107	0.00105
34	17809.0	18153.0	NA	NA	0.331	0.363	0.379	0.373	0.00104	0.00104
35	20984.0	22100.0	NA	NA	0.377	0.378	0.354	0.370	0.00100	0.00104
36	19091.0	20577.0	NA	NA	0.342	0.379	0.337	0.342	0.00111	0.00107
37	17392.0	18954.0	NA	NA	0.315	0.352	0.350	0.331	0.00097	0.00099
38	17829.0	18351.0	NA	NA	0.345	0.333	0.406	0.383	0.00100	0.00100
39	15221.0	15979.0	NA	NA	0.326	0.310	0.329	0.304	0.00109	0.00108
40	16087.0	15445.0	NA	NA	0.364	0.354	0.334	0.333	0.00104	0.00100
41	21903.0	22333.0	NA	NA	0.306	0.343	0.352	0.371	0.00107	0.00110
42	17517.0	18176.0	NA	NA	0.348	0.360	0.362	0.355	0.00106	0.00111
43	18730.0	19029.0	NA	NA	0.332	0.354	0.337	0.356	0.00097	0.00098
44	18927.0	18946.0	NA	NA	0.348	0.334	0.358	0.362	0.00104	0.00101
45	13996.0	14726.0	NA	NA	0.397	0.383	0.358	0.351	0.00099	0.00102
46	20454.0	21074.0	NA	NA	0.335	0.332	0.363	0.343	0.00104	0.00105
47	17963.0	17843.0	NA	NA	0.354	0.365	0.352	0.333	0.00104	0.00105
48	17661.0	17820.0	NA	NA	0.355	0.345	0.339	0.351	0.00105	0.00107
Mean	9218.5	9506.0	232.3±27.1	233.0±28.5	0.351	0.359	0.364	0.359	0.00104	0.00105
Standard error	1148.9	1195.5	5.5±0.7	5.2±0.7	6.7E-3	7.0E-3	5.7E-3	5.3E-3	8.9E-6	8.2E-6
p-value	0.86		0.25		0.42		0.55		0.60	

Notations: FA, fractional anisotropy; MD, mean diffusivity; NA, Not Available; StD, standard deviation; FLAIR, Fluid Attenuated Inversion Recovery;

Table 3

HVU and its 95% CI (HVU_L, HVU_U) estimated using control nonepileptic subjects for the listed lateralizing methods.

Imaging Attributes	Number of Subjects	HVU	HVU_L	HVU_U
Posteroinferior Cingulum FA	23	0.027	0.021	0.037
Crus fo Fornix FA	23	0.018	0.014	0.025
Hippocampal MD value	20	$\mathbf{3.1 \times 10^{-5}}$	$\mathbf{2.4 \times 10^{-5}}$	$\mathbf{4.5 \times 10^{-5}}$
Hippocampal Volume	45	0.069	0.058	0.087
Hippocampal FLAIR intensity	25	0.099	0.078	0.137

Table 4

Outcome of TLE lateralization methods.

				FA in Posteroinferior Cingulum			FA in Crus of Fornix			Hippocampal MD (mm^2 /s)			Hippocampal Volumetrics (mm^3)			Hippocampal FLIAR Intensity Mean±StD		
No	**P MTS**	**ECoG**	**Side**	**Left**	**Right**	**LAT**	**Left**	**Right**	**LAT**	**Left**	**Right**	**LAT**	**Left**	**Right**	**LAT**	**Left**	**Right**	**LAT**
1	Y	Y	L	0.412	0.453	L	0.272	0.347	L	1.3E-3	9.6E-4	L	1855.0	3578.3	L	277.7± 36.0	269.4±23.9	L
2	Y	N	L	0.299	0.342	L	0.232	0.296	L	1.1E-3	9.6E-4	L	1434.4	2373.0	L	218.4±38.4	195.0±26.6	L
3	Y	Y	L	0.415	0.451	L	0.323	0.459	L	1.3E-3	1.0E-3	L	2050.0	3614.8	L	252.2±35.0	233.8±25.7	L
4	Y	N	L	0.341	0.370	L	0.350	0.380	L	1.4E-3	1.1E-3	L	1641.5	3145.7	L	273.9±43.7	247.2±34.5	L
5	Y	N	L	0.268	0.353	L	0.260	0.284	L	1.6E-3	1.1E-3	L	1155.7	2003.5	L	468.6±78.0	444.6±57.0	L
6	Y	N	L	0.392	0.431	L	0.306	0.335	L	1.3E-3	1.1E-3	L	1926.8	2676.4	L	558.1±55.6	504.5±44.3	L
7	Y	N	L	0.400	0.505	L	0.390	0.392	U	1.2E-3	1.1E-3	L	1774.1	3003.4	L	314.2±33.5	299.2±26.8	L
8	Y	Y	R	0.370	0.292	R	0.356	0.337	R	1.4E-3	1.4E-3	R	2993.9	2390.1	U	338.9±27.4	347.4±43.5	R
9	Y	Y	R	0.272	0.192	R	0.276	0.176	R	9.6E-4	1.3E-3	R	2456.9	773.4	R	419.2 ±58.3	422.8±84.3	R
10	Y	N	R	0.400	0.371	R	0.365	0.322	R	1.0E-3	1.3E-3	R	2803.5	1955.4	R	295.0±26.7	294.4±42.9	R
11	N	N	L	0.412	0.458	L	0.332	0.351	L	1.4E-3	1.1E-3	L	1361.3	2806.5	L	212.3±43.2	212.4±27.2	L
12	N	N	L	0.307	0.380	L	0.310	0.313	U	1.2E-3	1.2E-3	L	2590.9	3370.5	U	252.5±27.1	238.9±27.9	U
13	N	N	L	0.401	0.435	L	0.351	0.359	U	1.1E-3	1.0E-3	L	1969.1	3407.6	L	236.1±30.4	230.2±27.3	L
14	N	N	R	0.341	0.327	U	0.342	0.319	R	1.1E-3	1.3E-3	R	2842.4	1923.8	R	196.8±26.8	207.0±37.3	R
15	N	N	R	0.296	0.253	R	0.292	0.099	R	1.2E-3	1.8E-3	R	1492.0	847.8	R	301.8±26.3	315.3±40.1	R
16	N	N	R	0.344	0.335	U	0.344	0.311	R	1.1E-3	1.1E-3	R	3254.3	2503.3	U	517.7±77.2	514.6±54.4	L
17	N	Y	R	0.304	0.322	U	0.259	0.282	L	1.2E-3	1.3E-3	R	1592.8	1922.2	U	507.9±57.1	500.7±68.3	R
18	N	Y	R	0.321	0.342	U	0.327	0.299	R	1.1E-3	1.1E-3	U	2097.8	1899.4	U	312.5±37.6	310.4±39.9	U
19	N	N	R	0.308	0.288	U	0.300	0.285	U	1.1E-3	1.1E-3	U	3001.8	3068.2	U	415.6±30.9	412.7±35.4	R
20	N	Y	R	0.349	0.322	R	0.337	0.388	L	1.1E-3	1.2E-3	R	2736.6	2979.3	U	407.7±41.3	416.5±35.5	L

The side of epileptogenicity is confirmed by postsurgical outcome (Engel classification). Mean FA in the posteroinferior cingulum and fornix crus, and mean hippocampal MD, along with hippocampal volumetrics and mean and standard deviation of FLAIR intensities are shown for left and right hemispheres for each TLE patient with the related putative lateralization of epileptogenicity.

Table notation: P MTS, Pathology-Proven Mesial Temporal sclerosis; StD, Standard Deviation, FA, Fractional Anisotropy; MD, Mean Diffusivity; FLAIR, Fluid Attenuated Inversion Recovery; Side, Side of Epileptogenicity; LAT, Lateralization of Epileptogenicity; Y, Yes; N, No; U, Uncertain Lateralization; L, Left; R, Right.